BPR MCS | Bulletin of Pioneering Researches of Medical and Clinical Science

Bulletin of Pioneering Researches of Medical and Clinical Science

Available online: https://bprmcs.com
2023 | Volume 3 | Issue 2 | Page: 121-133

Longitudinal Changes in Hemostatic Protein Cargo of LDL-Precipitated Extracellular Vesicles Are Superior to Conventional Biomarkers in Predicting Favorable Left Ventricular Remodeling Post-Myocardial Infarction

Carlos R. Mendoza[1]*, Li Wei[1], Ahmad K. El Sherif[1]

[1]Department of Clinical Sciences, National Autonomous University of Mexico, Mexico City, Mexico.

Abstract

A distinct group of plasma extracellular vesicles (EVs) that co-isolate with low-density lipoprotein (LDL-EVs) contains proteins involved in coagulation and fibrinolytic pathways. This work examined whether the balance between these hemostatic and fibrinolysis-related proteins within LDL-EVs corresponds to patterns of post-acute myocardial infarction (post-AMI) left ventricular (LV) remodeling, a process that can lead to heart failure. Levels of von Willebrand factor (VWF), SerpinC1, and plasminogen were quantified in LDL-EVs obtained from plasma at baseline (≤72 h after AMI), 1 month, and 6 months in a cohort of 198 individuals. Based on the 6-month change in LV end-systolic volume (≥15 increase vs. ≥15 decrease), participants were assigned to adverse (n = 98) or reverse (n = 100) remodeling categories. A multilevel longitudinal structural equation modeling (ML-SEM) framework was applied to determine predictive value independent of baseline status. At the baseline sampling point, LDL-EV cargo levels of VWF, SerpinC1, and plasminogen were comparable between the two remodeling groups. By 1 month in the adverse-remodeling group, VWF and SerpinC1 showed declines, while plasminogen rose. Conversely, in those showing reverse remodeling, VWF and plasminogen fell, with SerpinC1 showing no major change. Ultimately, compared with the adverse group, individuals with reverse remodeling displayed higher SerpinC1 and VWF but reduced plasminogen, yielding elevated VWF: Plasminogen and SerpinC1:Plasminogen ratios at both 1 and 6 months. Importantly, the ratios VWF: Plasminogen (AUC = 0.674) and SerpinC1: Plasminogen (AUC = 0.712) offered substantially better prognostic discrimination than NT-proBNP (AUC = 0.384), troponin-I (AUC = 0.467), or troponin-T (AUC = 0.389) ($p < 0.001$). Shifts over time in LDL-EV-associated coagulation/fibrinolysis ratios outperform established circulating biomarkers for forecasting post-AMI reverse remodeling. These results may help point to cellular mechanisms involved in structural recovery of the LV following AMI.

Keywords: Extracellular vesicles, Coagulation, Fibrinolysis, Acute myocardial infarction, Ventricular remodeling, Heart failure

Corresponding author: Carlos R. Mendoza
E-mail: carlos.mendoza@outlook.com

How to Cite This Article: Mendoza CR, Wei L, El Sherif AK. Longitudinal Changes in Hemostatic Protein Cargo of LDL-Precipitated Extracellular Vesicles Are Superior to Conventional Biomarkers in Predicting Favorable Left Ventricular Remodeling Post-Myocardial Infarction. Bull Pioneer Res Med Clin Sci. 2023;3(2):121-33. https://doi.org/10.51847/aYk8eR7pP6

Introduction

Although improvements in revascularization approaches and adjunctive drug therapy have reduced mortality from acute myocardial infarction (AMI) over the past several decades, heart failure (HF) arising from maladaptive ("adverse") post-AMI left ventricular (LV) remodeling still contributes substantially to global morbidity and

mortality [1]. Adverse remodeling is typified by progressive structural alterations such as thinning of peri-infarct and remote myocardium, expansion of ventricular mass and cavity size, and a shift from an elongated to a more spherical chamber shape, all of which ultimately impair contractile performance. Processes such as activation of inflammatory and coagulation cascades, fibrosis, and microvascular obstruction drive this maladaptive trajectory [2, 3]. In contrast, a subset of patients display reductions in LV volumes—termed "reverse" remodeling—which signal functional improvement and, combined with neurohormonal blockade, correspond to better clinical outcomes and lower HF progression rates [4, 5]. A commonly used echocardiographic benchmark to classify remodeling status is the 6-month change in LV end-systolic volume (LVESV), with a threshold of ±15% defining adverse (−) or reverse (+) remodeling [5, 6]. Given the inherent observer-dependent variability of echocardiographic volume measurements, pairing LVESV changes with relevant biological markers reflecting remodeling mechanisms may refine risk prediction and improve clinical decision-making for individuals at heightened risk of adverse structural evolution.

Extracellular vesicles (EVs) are lipid-bilayer particles loaded with molecular cargo—including proteins, lipids, RNAs, and microRNAs—derived from their parent cells and mirroring the physiological or pathological context at the time they are released [7]. EVs circulating in plasma have therefore become promising candidates for cardiovascular biomarker discovery [8–13]. After AMI, EVs shed from diverse cardiac cell types may participate in remodeling through cell-to-cell signaling [14–18], and circulating EV concentrations rise markedly following infarction [19–21]. EVs obtained from AMI patients are associated with microvascular obstruction, provoke endothelial dysfunction in vitro, and harbor prothrombotic components such as tissue factor and Serpin F2 [15, 20–22], suggesting that EV-mediated thrombogenicity may influence post-AMI remodeling. While earlier studies have offered cross-sectional views of EV profiles in AMI [14, 15, 19, 20], longitudinal tracking of EV dynamics across well-documented remodeling phases remains limited.

Our prior work identified, among EVs that co-precipitate with low-density lipoprotein (LDL), a subset enriched with procoagulant proteins (LDL-EVs) [23]. In this study, we evaluate whether time-dependent shifts in LDL-EV hemostatic protein content—and particularly the ratios between coagulation-related and fibrinolytic components—are linked to patterns of LV remodeling after AMI (primary outcome), given their potentially divergent effects on infarct healing and scar maturation. Secondary aims include (1) examining clinical correlations between LDL-EV protein ratios and variables in adverse versus reverse remodeling groups, and (2) assessing the prognostic capability of these ratios for predicting remodeling trajectories following AMI.

Materials and Methods

Study framework and participants

This investigation was conducted as a nested case–control study, pairing individuals with adverse LV remodeling against those exhibiting reverse LV remodeling, drawn from the IMMACULATE registry **(Figure 1)** [24, 25]. The registry encompassed multiple centers. Inclusion criteria for participants in this analysis were: documented ischemic chest pain lasting >30 minutes, corresponding ECG changes, cardiac troponin levels exceeding the 99th percentile upper reference limit, and angiographic evidence of ≥50% stenosis in at least one coronary artery. Exclusion criteria included age >85 years, presence of valvular heart disease, cardiogenic shock, active malignancy, severe renal dysfunction (eGFR <15 mL/min/1.73 m²), liver disease, anemia, HIV infection, or hepatitis B/C.

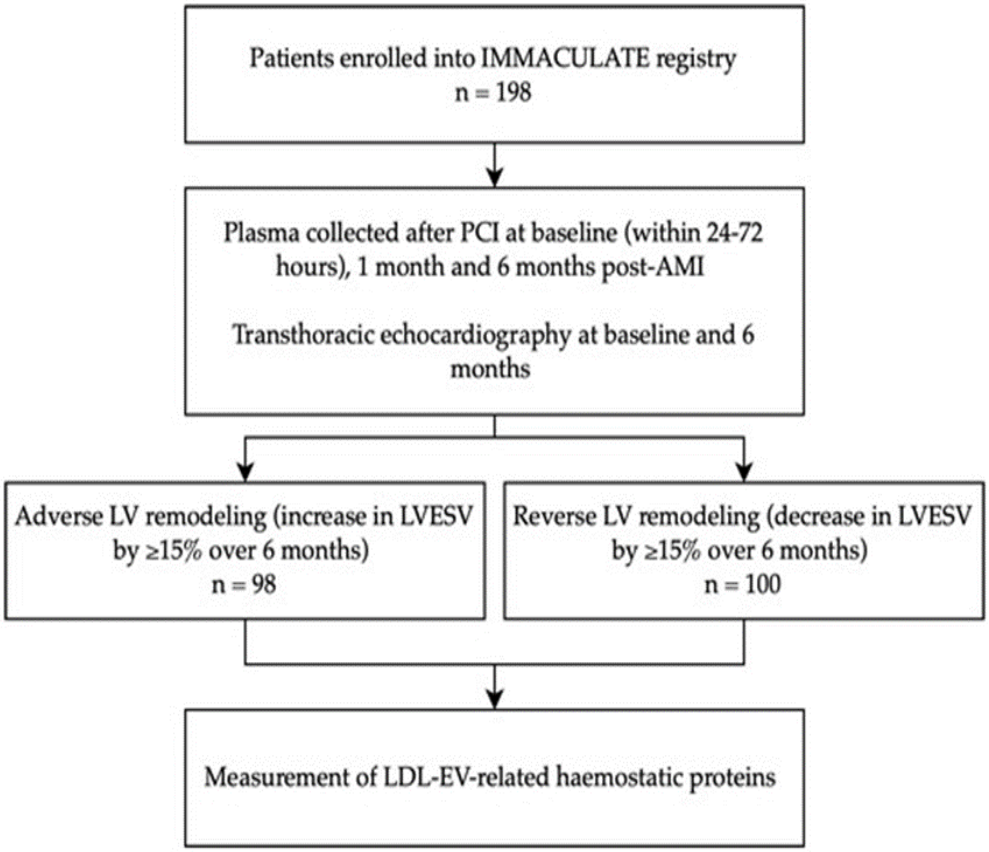

Figure 1. Schematic of study design. Abbreviations: PCI, percutaneous coronary intervention; LVESV, left ventricular end-systolic volume.

Peripheral blood was drawn at three time points: within 24–72 h post-PCI (baseline), 1 month, and 6 months post-AMI. Samples were processed by centrifugation, and plasma aliquots were stored at −80 °C until assays for NT-proBNP, hsTnT, hsTnI, and LDL-EV isolation. Echocardiographic evaluations were performed at baseline and 6 months. Based on LVESV change over 6 months [5, 6], patients were assigned to two groups: adverse LV remodeling (n = 98, >15% LVESV increase) or reverse LV remodeling (n = 100, >15% LVESV reduction). Participants were monitored for up to 2 years for MACCEs, including cardiovascular mortality, HF, recurrent MI, and ischemic stroke. HF diagnoses followed European Society of Cardiology criteria, confirmed by an emergency medicine physician and a cardiologist [1]. All subjects signed informed consent. The study protocol was approved by the National University of Singapore IRB (NHG DSRB Ref: 2015/01156) and adhered to the Declaration of Helsinki.

LDL-EV isolation

LDL-EVs were prepared following a previously published protocol [23]. Dextran sulfate (DS, 6.5% w/v) and 2 M $MnCl_2$ stock solutions were made. DS (1:125 v/v) and $MnCl_2$ (1:40 v/v) were sequentially added to 125 µL plasma, gently mixed, and centrifuged at 4800 g for 10 minutes at 4 °C. The resulting pellets (LDL-EV fractions) were either resuspended for characterization or lysed in 125 µL lysis buffer (Roche #04719956001) for protein analysis, and stored at −80 °C.

LDL-EV characterization

LDL-EVs were suspended in filtered PBS. Particle size and concentration were assessed by NTA (NanoSight NS300™, Malvern Instruments, UK). Five 60-s videos per sample were recorded at 25 °C at camera levels 11, 13, or 14, and analyzed with a detection threshold of 5–7. Zeta potential measurements were performed in duplicates at 25 °C using Litesizer 500 (Anton-Paar, Graz, Austria).

For TEM, 20 µL LDL-EVs were fixed in 2.5% glutaraldehyde for 1 hour at 4 °C, applied to Formvar Film 200 mesh CU grids, incubated 30 min, stained with 5% gadolinium triacetate for 1 min, and imaged at room temperature using FEI Tecnai G2 Spirit TEM (FEI, Hillsboro, OR, USA).

Quantitative protein measurement

Protein content was quantified using bead-based multiplex immunoassays [23]. Luminex MagPlex-C Microspheres (MC100-xx) were conjugated with capture antibodies. Samples were incubated with antibody-coupled beads and biotinylated detection antibodies, followed by addition of streptavidin-phycoerythrin (SA-PE, BD #554061) for quantification. Standard curves from recombinant proteins

were used to calculate concentrations. Measurements were performed on the Bio-Plex® 200 System (Bio-Rad #171-000201).

The reagents used included:

- VWF: recombinant human VWF (Factor VIII-free, Fitzgerald #30C-CP4003U), anti-human VWF (Fitzgerald #70R-10589), biotinylated anti-human VWF (Fitzgerald #60R-1019)
- SerpinC1: anti-thrombin III (NOVUS #NBP1-05149), biotinylated SerpinC1 (R&D #BAF1267), recombinant SerpinC1 (R&D #1267-PI-010)
- Plasminogen: anti-human plasminogen (NOVUS NB120-10176), biotinylated anti-plasminogen (NB120-10177), recombinant plasminogen (R&D 1939-SE-200)
- SerpinF2: anti-human SerpinF2 (R&D #MAB1470), biotinylated anti-SerpinF2 (R&D #BAF1470), recombinant SerpinF2 (R&D #1470-PI-010)

Statistical methods

Data are expressed as mean ± standard deviation (SD), median with interquartile range (IQR), or percentages as appropriate. Initial comparisons were conducted using unpaired Student's t-test or Mann–Whitney U test. Within-group changes from baseline to follow-up were evaluated with the Wilcoxon signed-rank test. The primary confirmatory analyses employed multilevel structural equation modeling (ML-SEM) and analysis of covariance (ANCOVA) to examine differences in LDL-EV protein content between adverse and reverse remodeling groups, with adjustment for baseline covariates (age, sex, ethnicity, diabetes mellitus, hypertension, dyslipidemia, lipid parameters, and concomitant medications). This modeling approach was selected to accommodate the repeated-measures design and the study hypotheses. Receiver operating characteristic (ROC) curves were generated to determine the discriminatory performance of individual LDL-EV protein ratios, as well as their combinations with conventional cardiac biomarkers and clinical parameters, for identifying reverse LV remodeling. Time-to-rehospitalization for heart failure according to remodeling status was displayed using Kaplan–Meier curves and compared with the log-rank test. A two-sided p-value < 0.05 was considered statistically significant. Analyses were performed using SPSS version 25.0 (IBM Corp., Armonk, NY, USA) and Stata/MP 16.0 (StataCorp, College Station, TX, USA).

Results and Discussion

Patient cohort

Baseline demographic and clinical features are displayed in **Table 1**. The cohort consisted of 198 patients, of whom 98 demonstrated adverse LV remodeling and 100 exhibited reverse LV remodeling, defined by a ≥15% increase or decrease, respectively, in LV end-systolic volume (LVESV) during the initial 6 months after AMI **(Figure 1)**. No significant intergroup differences were observed in age, sex, ethnicity, prior medical history, discharge diagnoses, medication profiles, or baseline lipid values. The only exception was a higher prevalence of warfarin use in the adverse remodeling group (11.2% vs. 2.0%; p = 0.009).

Table 1. Baseline characteristics of the study population.

	Adverse LV Remodeling n = 98	Reverse LV Remodeling n = 100	p-Value
Demographics			
Age, mean (years)	55 (48–60)	54 (49–62)	0.963
Male gender (%)	93 (94.9)	93 (93.0)	0.576
Ethnicity			
Chinese (%)	54 (55.1)	56 (56.0)	0.130
Malay (%)	26 (26.5)	16 (16.0)	
Indian (%)	14 (14.3)	25 (25.0)	
Others (%)	4 (4.1)	3 (3.0)	
Smoking status			
Never smoker (%)	28 (28.6)	32 (32.0)	0.869
Current smoker (%)	60 (61.2)	58 (58.0)	
Former smoker (%)	10 (10.2)	10 (10.0)	
Past medical history			

Diabetes mellitus (%)	20 (20.4)	20 (20.0)	0.943
Dyslipidaemia (%)	43 (43.9)	46 (46.0)	0.764
Hypertension (%)	44 (44.9)	40 (40.0)	0.486
Baseline lipid profile			
Total cholesterol (mmol/L)	5.43 (1.4)	5.43 (1.3)	1.000
HDL cholesterol (mmol/L)	1.03 (0.9–1.3)	1.10 (0.9–1.3)	0.647
LDL cholesterol (mmol/L)	3.54 (1.2)	3.50 (1.3)	0.820
Triglycerides (mmol/L)	1.56 (1.2–2.4)	1.64 (1.1–2.4)	0.691
Index diagnosis			
STEMI (%)	82 (83.7)	78 (78.0)	0.311
NSTEMI (%)	16 (16.3)	22 (22.0)	
Discharge medications			
Aspirin (%)	95 (96.9)	98 (98.0)	0.634
P2Y12 inhibitor (%)	95 (96.9)	99 (99.0)	0.303
Statin (%)	96 (98.0)	98 (98.0)	0.984
Warfarin (%)	11 (11.2)	2 (2.0)	0.009
Echocardiographic parameters at 6 months			
Δ LVEDV (%)	29.88 (18.3)	−12.26 (13.5)	<0.001
Δ LVESV (%)	29.43 (20.7–40.1)	−25.59 (−32.03–20.19)	<0.001
Δ LVEF (%)	−2.85 (−10.1–2.9)	16.43 (6.8–28.4)	<0.001

*Footnotes for **Table 1**:* Continuous variables are shown as mean ± SD or median (IQR); comparisons used unpaired t-test or Mann–Whitney U test. Categorical data are reported as percentages; group differences were tested with χ^2 test. Abbreviations: AMI, acute myocardial infarction; LV, left ventricular; HDL, high-density lipoprotein; LDL, low-density lipoprotein; STEMI, ST-elevation myocardial infarction; NSTEMI, non-ST-elevation myocardial infarction; LVEDV, left ventricular end-diastolic volume; LVESV, left ventricular end-systolic volume; EF, ejection fraction.

Conventional cardiac biomarkers in plasma

Serial measurements of NT-proBNP, high-sensitivity troponin T (hsTnT), and high-sensitivity troponin I (hsTnI) revealed a decline over the 6-month period in both remodeling groups **(Table 2)**. Patients with adverse remodeling exhibited higher baseline hsTnT and hsTnI concentrations, as well as elevated NT-proBNP and hsTnT levels at the 1-month and 6-month visits compared with the reverse remodeling group.

Table 2. Temporal profile of standard cardiac biomarkers in the study cohort.

Cardiac Biomarkers	Adverse LV Remodeling (n = 98)			Reverse LV Remodeling (n = 100)	
	Baseline	1 month	6 months	Baseline	1 month
NT-proBNP (pg/mL)	818.65 (397.50–1815.00)	614.00 (225.00–1285.00) **	205.85 (64.53–468.50) ***	789.95 (367.30–1202.00)	383.60 (143.25–697.50)
hsTnT (ng/L)	2807.00 (979.50–4406.00) ***	15.68 (9.79–23.09) **	10.37 (7.25–15.73) **	1578.50 (605.75–2632.00)	12.04 (7.83–16.62)
hsTnI (ng/L)	23219.40 (7359.60–43056.90) ***	12.70 (6.90–20.10)	7.45 (4.3–13.60)	9782.45 (3285.80–21938.75)	10.65 (5.90–19.35)

*Footnotes for **Table 2**:* Values are median (IQR). Between-group differences at each time point are denoted as **$p \leq 0.01$; ***$p \leq 0.001$. Abbreviations: AMI, acute myocardial infarction; LV, left ventricular; NT-proBNP, N-terminal pro-B-type natriuretic peptide; hsTnT, high-sensitivity troponin T; hsTnI, high-sensitivity troponin I.

Characterization of circulating LDL-associated extracellular vesicles

LDL-precipitated extracellular vesicles (LDL-EVs) isolated at baseline were characterized by transmission electron microscopy (TEM), nanoparticle tracking analysis (NTA), and Litesizer 500 assessment.

Longitudinal evolution of hemostatic proteins in LDL-EVs and relation to post-AMI LV remodeling

Temporal trajectories of three key hemostatic proteins carried by LDL-EVs—von Willebrand factor (VWF), SerpinC1 (antithrombin III), and plasminogen—were examined **(Figure 2a)**. In the adverse remodeling group, VWF concentrations progressively decreased throughout the 6-month follow-up, whereas in the reverse remodeling group the decline was confined to the first month **(Figure 2b)**. SerpinC1 levels dropped sharply by 1 month and remained suppressed at 6 months in adverse remodelers but stayed stable in reverse remodelers **(Figure 2c)**. Plasminogen showed the opposite pattern: it rose by 1 month and stayed elevated at 6 months in adverse remodeling patients, whereas it fell early and remained low in the reverse remodeling cohort **(Figure 2d)**. At individual time points, patients with adverse remodeling displayed significantly lower VWF (at 6 months), lower SerpinC1 (at 1 and 6 months), and higher plasminogen (at 1 and 6 months) in LDL-EVs compared with those exhibiting reverse remodeling.

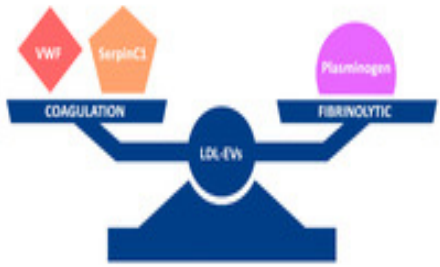

a)

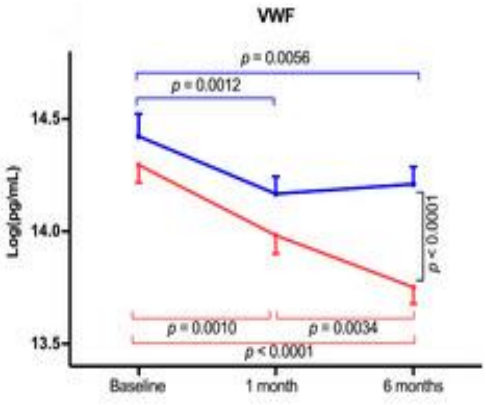

b)

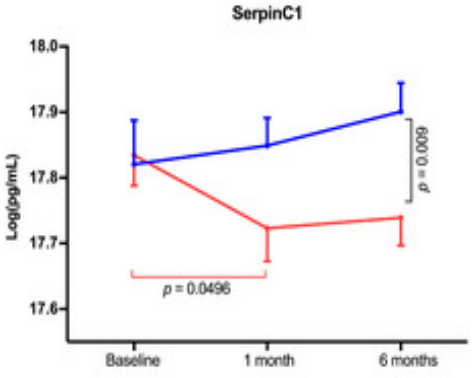

c)

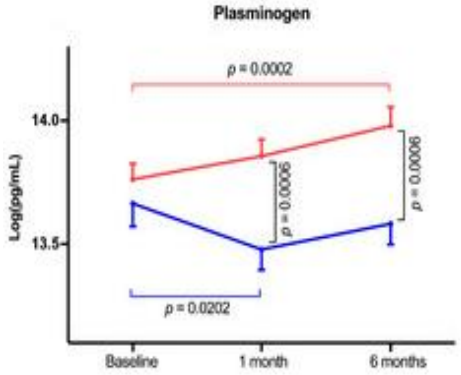

d)

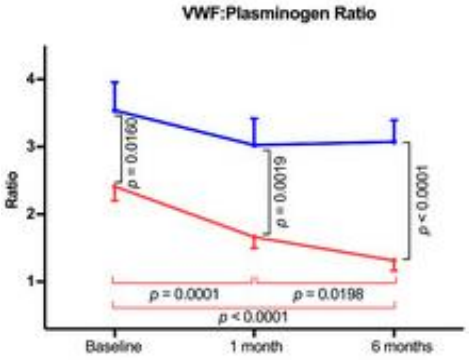

e)

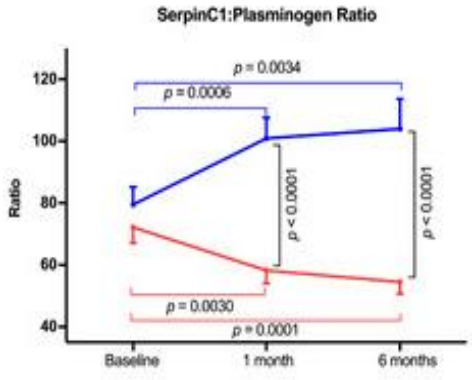

f)

Figure 2. Changes over Time in LDL-EV Hemostatic Proteins in Post-AMI Patients

We measured coagulation proteins (VWF, SerpinC1) and the fibrinolytic protein plasminogen, along with their respective ratios (VWF: Plasminogen, SerpinC1:Plasminogen), in LDL-EVs from 198 patients following AMI at baseline, 1 month, and 6 months **(Figure 2a)**. Panels B–F illustrate these measurements. Differences between baseline and follow-up within each group were assessed using the Wilcoxon signed-rank test (horizontal bars), while Mann–Whitney U tests were applied to compare adverse versus reverse LV remodeling groups (vertical bars). Values are shown as mean ± SEM. Because post-AMI remodeling involved shifts between coagulation- and fibrinolysis-related proteins, we analyzed how the ratios of VWF and SerpinC1 to plasminogen changed over time. In the adverse LV remodeling group, VWF: Plasminogen gradually decreased over 6 months, whereas in the reverse LV remodeling group it remained largely stable **(Figure 2e)**. SerpinC1:Plasminogen in the adverse group dropped within the first month and stayed low through month 6 **(Figure 2f)**. In contrast, SerpinC1:Plasminogen rose in the reverse remodeling group during the first month and remained elevated at 6 months relative to baseline. Comparing the groups, both ratios were substantially lower at 1 and 6 months in patients with adverse remodeling versus those with reverse remodeling.

ML-SEM modeling of LDL-EV protein ratios and LV remodeling

To determine if LDL-EV protein ratios could predict LV remodeling independent of baseline characteristics, we applied multilevel structural equation modeling (ML-SEM), which allows for interactions among variables **(Table 3)**. Patients exhibiting reverse LV remodeling had consistently higher VWF: Plasminogen and SerpinC1:Plasminogen ratios than those with adverse remodeling throughout the 6-month follow-up. These differences remained significant after controlling for age, sex, ethnicity, medications, lipid levels, and cardiovascular risk factors.

Table 3. ML-SEM Analysis of LDL-EV Protein Ratios

Outcome: Ratios of Coagulation and Fibrinolytic Proteins in LDL-Derived Extracellular Vesicles						
Predictor Variables	VWF : Plasminogen Ratio Coefficient	p-Value	95% CI	SerpinC1 : Plasminogen Ratio Coefficient	p-Value	95% CI
Demographics						
Age (years)	0.054	<0.001	(0.025 – 0.083)	−0.104	0.778	(−0.829 – 0.620)
Female sex	0.535	0.314	(−0.507 – 1.576)	26.449	0.047	(0.340 – 52.558)
Ethnicity (Reference: Chinese)						
Malay	−0.171	0.582	(−0.779 – 0.437)	−16.436	0.048	(−31.780 – −1.093)
Indian	0.017	0.957	(−0.602 – 0.635)	−13.950	0.092	(−29.302 – 1.402)
Other	0.342	0.645	(−1.112 – 1.800)	−25.197	0.179	(−61.956 – 11.563)
Smoking status (Reference: Never smoker)						
Current smoker	0.320	0.264	(−0.241 – 0.882)	10.312	0.148	(−3.652 – 24.277)
Former smoker	−0.126	0.780	(−1.008 – 0.757)	16.523	0.142	(−5.557 – 38.602)
Medical history						
Diabetes mellitus	−0.445	0.196	(−1.120 – 0.230)	1.367	0.875	(−15.632 – 18.365)
Dyslipidaemia	0.445	0.115	(−0.109 – 1.000)	8.560	0.277	(−5.332 – 22.453)
Hypertension	−0.089	0.755	(−0.652 – 0.473)	2.808	0.694	(−11.192 – 16.809)
Baseline lipid profile						
Total cholesterol (mmol/L)	−0.457	0.061	(−0.935 – 0.022)	−2.235	0.715	(−14.228 – 9.759)
HDL cholesterol (mmol/L)	0.119	0.816	(−0.882 – 1.120)	14.953	0.240	(−9.974 – 39.880)
LDL cholesterol (mmol/L)	0.565	0.035	(0.038 – 1.092)	−1.813	0.788	(−15.041 – 11.415)
Triglycerides (mmol/L)	0.061	0.319	(−0.059 – 0.181)	−0.527	0.731	(−3.531 – 2.477)
Discharge medications						
Aspirin	−2.397	0.004	(−4.008 – −0.786)	−4.483	0.828	(−44.926 – 35.959)
P2Y12 inhibitor	−1.970	0.054	(−3.977 – 0.037)	−15.068	0.560	(−65.690 – 35.553)

Statin	−2.889	0.002	(−4.737 – −1.040)	29.643	0.213	(−17.047 – 76.332)
Warfarin	−0.774	0.172	(−1.886 – 0.338)	−12.604	0.378	(−40.601 – 15.393)
Time point of protein measurement (Reference: 1 month)						
Baseline	0.416	<0.001	(0.344 – 0.488)	0.647	<0.001	(0.537 – 0.757)
6 months	−0.164	0.478	(−0.616 – 0.288)	−0.472	0.935	(−11.780 – 10.854)
Pattern of LV remodeling (Reference: Adverse remodeling)						
Reverse remodeling (model a)	1.093	<0.001	(0.613 – 1.573)	41.448	<0.001	(30.363 – 52.533)
Reverse remodeling (model b)	1.122	<0.001	(0.640 – 1.604)	40.698	<0.001	(28.786 – 52.611)

Footnotes for **table 3**: [a] Adjusted for protein level changes; b Adjusted for protein level changes, age, sex, ethnicity, comorbidities, baseline lipids, and medication use. Bold indicates $p < 0.05$.

ANCOVA post hoc analysis confirmed that the divergence in these ratios between reverse and adverse remodeling groups was already evident at 1 month and persisted through 6 months post-AMI.

Clinical associations of LDL-EV protein ratios

Backward-elimination ML-SEM was used to explore clinical factors associated with LDL-EV protein ratios in both remodeling groups. Fourteen variables—including age, sex, ethnicity, comorbidities, cardiovascular risk factors, and treatments—were evaluated **(Table 3)**. The VWF: Plasminogen ratio correlated significantly with age, LDL cholesterol, aspirin, and statin use. SerpinC1: Plasminogen ratio was linked to sex and Malay ethnicity. Critically, both ratios were independently associated with reverse LV remodeling after AMI, even after accounting for other cardiovascular risk variables.

LDL-EV protein ratios as predictors for LV remodeling and heart failure

To assess prognostic value, we compared VWF: Plasminogen and SerpinC1:Plasminogen ratios with conventional cardiac biomarkers at 1 month post-AMI **(Table 4 and Figure 3a)**. Standard markers—NT-proBNP (AUC = 0.384), hsTnI (AUC = 0.467), hsTnT (AUC = 0.389)—showed limited ability to discriminate reverse from adverse remodeling. In contrast, VWF: Plasminogen and SerpinC1: Plasminogen exhibited stronger predictive performance, with AUCs of 0.674 and 0.712, respectively. Using Delong's test [26], VWF: Plasminogen AUC exceeded NT-proBNP ($Z = 5.281$, $p < 0.001$), hsTnI ($Z = 3.604$, $p < 0.001$), and hsTnT ($Z = 5.215$, $p < 0.001$). Likewise, SerpinC1: Plasminogen outperformed NT-proBNP ($Z = 6.130$, $p < 0.001$), hsTnI ($Z = 4.350$, $p < 0.001$), and hsTnT ($Z = 5.668$, $p < 0.001$). These results indicate that the coagulation-to-fibrinolysis protein ratios provide superior prediction of reverse LV remodeling compared with conventional cardiac injury biomarkers.

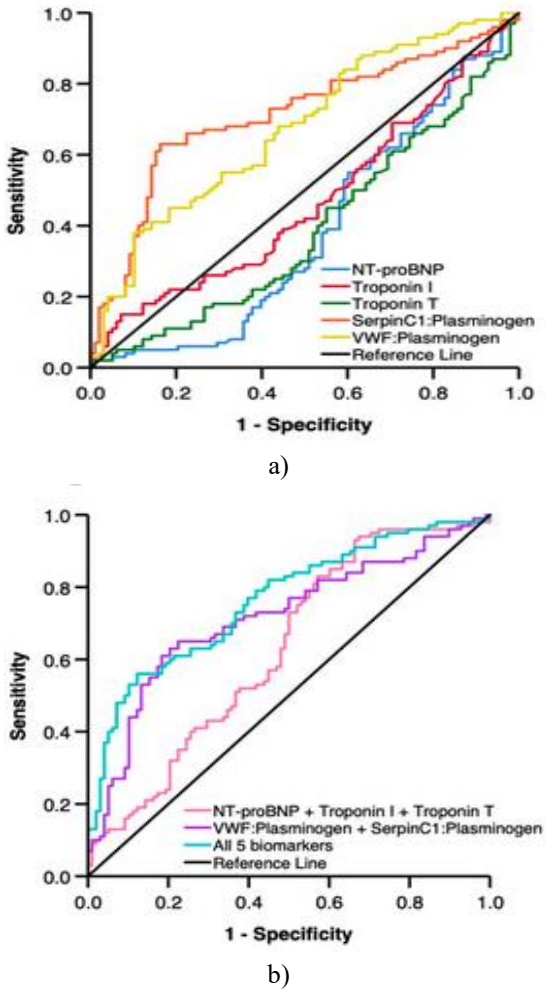

Figure 3. Receiver operating characteristic (ROC) curves for the identification of reverse left ventricular remodeling at 1 month after acute myocardial infarction.

(a) Individual performance of conventional cardiac injury biomarkers and LDL-EV–derived coagulation/fibrinolysis protein ratios at 1 month post-AMI.

(b) Performance of the combined model integrating LDL-EV protein ratios with the three cardiac injury biomarkers at 1 month post-AMI.

Table 4. Area under the ROC curve (AUC) values for various candidate predictors of reverse left ventricular remodeling.

Biomarker(s)	Area Under the Curve (AUC)	95% Confidence Interval	p-Value
NT-proBNP	0.384	0.305 – 0.463	0.005
hsTnI	0.467	0.386 – 0.548	0.419
hsTnT	0.389	0.311 – 0.467	0.007
VWF : Plasminogen ratio	0.674	0.599 – 0.748	<0.001
SerpinC1 : Plasminogen ratio	0.712	0.639 – 0.786	<0.001
Combined NT-proBNP + hsTnI + hsTnT	0.628	0.550 – 0.706	0.002
Combined VWF:Plasminogen + SerpinC1:Plasminogen	0.717	0.645 – 0.790	<0.001
All five biomarkers combined	0.763	0.697 – 0.829	<0.001

The predictive accuracy of integrating LDL-EV protein ratios with the standard cardiac injury markers was then evaluated **(Table 4 and Figure 3b)**. Three prognostic models were directly compared using ROC analysis:
(1) cardiac injury biomarker panel alone (NT-proBNP + hsTnI + hsTnT);
(2) LDL-EV protein ratio panel alone (VWF: Plasminogen + SerpinC1:Plasminogen);
(3) combined model (LDL-EV ratios + cardiac injury panel).
The AUC for the LDL-EV ratio panel was 0.717 and for the cardiac injury panel was 0.628, with no significant difference between them. However, the combined model yielded a significantly superior AUC of 0.763 compared with the cardiac injury panel alone (Z = 3.152, p = 0.002). Over a median follow-up duration of 2 years (IQR 1.9–2 years), heart failure was diagnosed in 11 of 98 patients (11.3%) with adverse LV remodeling versus 3 of 100 patients (3.0%) with reverse LV remodeling (p = 0.025; **(Figure 4)**).

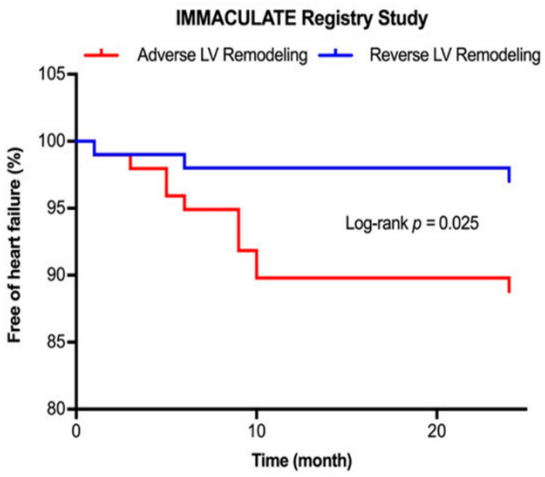

Figure 4. Cumulative incidence of heart failure during long-term follow-up. Kaplan–Meier curves showing time to rehospitalization for heart failure according to post-AMI left ventricular remodeling status.

Extracellular vesicles (EVs) circulating in plasma after myocardial injury can provide a snapshot of ongoing myocardial pathophysiology and may serve as surrogate biomarkers for predicting LV remodeling. The coagulation and fibrinolysis systems, tightly regulated under physiological conditions, are key mediators of inflammation and play a crucial role in tissue remodeling. In this study, we analyzed temporal variations in coagulation proteins (VWF, SerpinC1) and fibrinolytic protein (plasminogen), along with their ratios (VWF: Plasminogen and SerpinC1:Plasminogen), in LDL-EVs from post-AMI patients exhibiting either adverse or reverse LV remodeling. Our results indicate that elevated coagulation proteins and reduced fibrinolytic protein levels in LDL-EVs were independently linked to reverse LV remodeling. Importantly, the dynamics of coagulation-to-fibrinolysis protein ratios in LDL-EVs predicted reverse LV remodeling more accurately than conventional plasma biomarkers (NT-proBNP, hsTnI, hsTnT). To our knowledge, this is the first report linking EV-associated hemostatic protein levels to post-AMI LV remodeling. While our observational design does not define the precise underlying mechanisms, it supports the notion that inflammatory and coagulation processes are central to post-infarct LV remodeling.
Cardiac remodeling involves multiple pathophysiological changes following myocardial injury. The higher baseline plasma troponin T levels observed in patients with adverse LV remodeling **(Table 2)** suggest greater initial myocardial damage, which may contribute to subsequent maladaptive LV changes [27]. In addition to direct myocardial injury, maladaptive remodeling involves altered metabolic processes, including increased glucose oxidation coupled with reduced fatty acid utilization, modifications in the extracellular matrix, altered gene expression, neurohormonal dysregulation, and cardiomyocyte loss [27]. Previously considered largely irreversible and linked to poor outcomes [28], post-infarct remodeling is now recognized as partially reversible with appropriate therapeutic interventions [27]. For example,

LV assist device (LVAD) therapy promotes reverse remodeling via mechanical unloading, improving hemodynamics, cardiac output, and neurohormonal profiles [29, 30]. Nevertheless, whether myocardial energy metabolism fully normalizes during reverse remodeling remains unclear. Furthermore, changes in microRNA and long non-coding RNA profiles have been observed after LVAD support and may help evaluate HF severity [31–33], though their utility as remodeling biomarkers is not yet established. Our analysis of hemostatic protein composition in LDL-EVs shows that temporal changes in coagulation-to-fibrinolysis ratios can predict reverse LV remodeling as early as 1 month post-AMI. This may allow earlier detection than the 6-month echocardiographic assessment, facilitating timely therapeutic interventions to protect myocardial function [34].

VWF, a central coagulation protein, promotes thrombus formation by facilitating platelet adhesion and aggregation and serves as a carrier for factor VIII [35, 36]. Plasma VWF typically peaks 48–72 hours after AMI [37]. In line with previous studies, we observed the highest LDL-EV VWF levels at 3 days post-AMI, followed by a decline by 1 month in both remodeling groups. By 6 months, patients with adverse LV remodeling had significantly lower LDL-EV VWF levels compared with those exhibiting reverse remodeling. Although counterintuitive—given VWF's role in leukocyte recruitment and inflammation [38, 39]—this may reflect sequestration of VWF within LDL-EVs as part of a homeostatic response during remodeling.

SerpinC1 (antithrombin III) inhibits thrombin and other serine proteases (IXa, Xa, XIa, XIIa) [40] and exerts anti-inflammatory effects via coagulation-dependent and independent mechanisms [41, 42]. Elevated SerpinC1 in LDL-EVs from patients with reverse LV remodeling may indicate its protective, anti-inflammatory role in cardiac repair. Conversely, plasminogen, the precursor of plasmin, mediates fibrinolysis activated by tPA and uPA [43, 44]. Higher LDL-EV plasminogen in adverse remodeling patients may enhance TLR-4 formation, activate fibrin degradation products, or stimulate matrix metalloproteinases, releasing matrix-bound growth factors [45, 46]. Plasmin-mediated PAR-1 activation [47] may further drive pro-inflammatory and pro-remodeling pathways, potentially contributing to adverse LV remodeling.

Evaluating VWF: Plasminogen and SerpinC1:Plasminogen ratios in LDL-EVs revealed that higher coagulation-to-fibrinolysis ratios correlate with reverse LV remodeling. ML-SEM modeling further highlighted associations between these ratios and clinical variables. Metabolic abnormalities such as hyperglycemia, hyperlipidemia, and hypercholesterolemia can induce endothelial dysfunction via increased reactive oxygen species and reduced nitric oxide, elevating plasma VWF [48, 49]. Consistent with this, LDL-EV VWF: Plasminogen ratios correlated positively with LDL cholesterol. No significant associations were observed with hypertension, contrasting with prior plasma-based studies [50]. These differences between plasma and EV VWF may offer mechanistic insights into cardiovascular pathophysiology and warrant further investigation. Moreover, patients on statin therapy exhibited lower LDL-EV VWF: Plasminogen ratios, aligning with prior work linking rosuvastatin treatment to LDL-EV VWF and plasminogen levels [51].

The SerpinC1:Plasminogen ratio within LDL-EVs was markedly lower in women compared with men. This observation points toward sex-specific pathophysiological pathways after myocardial infarction. Although women typically present with less obstructive coronary disease and better-preserved left ventricular function following AMI [52, 53], they paradoxically experience higher post-MI mortality and worse long-term outcomes than men. Emerging evidence attributes this disparity to impaired coronary vasoreactivity, coronary microvascular dysfunction, and increased microembolization in female patients [52–54]. Additional contributing elements may include fluctuating reproductive hormone profiles, heightened adrenergic tone via the autonomic nervous system, and a greater clustering of atherogenic risk factors in women [55]. These sex-related biological differences likely underlie the distinct LDL-EV protein signatures observed between male and female participants in the present cohort.

Limitations

1. As a hypothesis-generating proof-of-concept investigation, we deliberately enrolled two extreme phenotypic groups defined by unequivocal 6-month echocardiographic remodeling patterns. External validation in independent, larger cohorts is essential. Given the male predominance in our study—consistent with the higher incidence of AMI in men [55, 56]—dedicated evaluation in female-predominant or female-only cohorts is strongly encouraged.
2. Pre-hospital and periprocedural (acute-phase) plasma samples were unavailable, precluding assessment of LDL-EV protein dynamics immediately before or at the exact moment of infarction. Similarly, parallel measurements of circulating free (non-EV) VWF, SerpinC1, and plasminogen were not performed; such data could clarify the exchange mechanisms between soluble and EV-encapsulated pools and strengthen mechanistic interpretation.

3. Due to resource constraints, comprehensive LDL-EV characterization (beyond size, zeta potential, and concentration) was limited to baseline samples only. However, the core findings rely on longitudinal changes in cargo protein content rather than vesicle biophysics, minimizing the impact of this restriction.
4. The current analysis focused on only three hemostatic proteins; the prognostic relevance of the broader LDL-EV proteome in post-infarction remodeling remains unexplored.
5. Mechanistic insight into how LDL-EV–associated hemostatic proteins actively contribute to ventricular remodeling requires dedicated preclinical models.

Conclusion

Ratios of coagulation-to-fibrinolysis proteins carried by circulating LDL-associated extracellular vesicles substantially outperform conventional plasma biomarkers in forecasting favorable (reverse) left ventricular remodeling after acute myocardial infarction. Serial alterations in the hemostatic protein profile of LDL-EVs emerge as a promising biomarker platform for monitoring post-AMI ventricular remodeling trajectories. These findings offer a clinically accessible window into underlying cellular processes and may ultimately inform targeted therapeutic strategies aimed at preventing progression to heart failure.

Acknowledgments: None

Conflict of interest: None

Financial support: This work was supported by the National University Health System (NUHS O-CRG 23 October 2016; NUHSRO/2018/095/RO5+5/Seed-Nov/05), the Singapore Ministry of Health's National Medical Research Council (MOH-OFIRG21nov-0010), the NUS NanoNASH Program (NUHSRO/2020/002/NanoNash/LOA), and the NUS Yong Loo Lin School of Medicine Nanomedicine Translational Research Program (NUHSRO/2021/034/TRP/09/Nanomedicine) to J.W.W.; NMRC (NMRC CG21APR1008) to A.M.R., M.Y.C. and J.W.W.; National Science Foundation (NSF/IRES/1559445) to C.L.H.; S.Y.C. would like to thank the generous support from the ESR/Teng GL PhD Scholarship program; C.H. would like to acknowledge the PhD Scholarship from Singapore Ministry of Education to support his study at NUS.

Ethics statement: The study was approved by National University of Singapore Institutional Research Board (NHG DSRB Ref: 2015/01156) and was conducted in accordance with the principles of the Declaration of Helsinki.

Informed consent was obtained from all subjects involved in the study.

References

1. Ponikowski P, Voors AA, Anker SD, Bueno H, Cleland JGF, Coats AJS, et al. 2016 ESC Guidelines for the diagnosis and treatment of acute and chronic heart failure. Eur J Heart Fail. 2016;18(8):891–975.
2. French BA, Kramer CM. Mechanisms of postinfarct left ventricular remodeling. Drug Discov Today Dis Mech. 2007;4(3):185–96.
3. Chong AY, Lip GYH. The prothrombotic state in heart failure. Eur J Heart Fail. 2007;9(2):124–8.
4. Bhatt AS, Ambrosy AP, Velazquez EJ. Adverse and reverse remodeling after myocardial infarction. Curr Cardiol Rep. 2017;19(8):71.
5. Waring AA, Litwin SE. Redefining reverse remodeling. J Am Coll Cardiol. 2016;68(12):1277–80.
6. Stellbrink C, Breithardt OA, Franke A, Sack S, Bakker P, Auricchio A, et al. Impact of cardiac resynchronization therapy on left ventricular remodeling. J Am Coll Cardiol. 2001;38(7):1957–65.
7. Tkach M, Théry C. Communication by extracellular vesicles. Cell. 2016;164(6):1226–32.
8. Wang JW, Gijsberts CM, Seneviratna A, de Hoog VC, Vrijenhoek JEP, Schoneveld AH, et al. Plasma extracellular vesicle protein content. Neth Heart J. 2013;21(10):467–71.
9. Boulanger CM, Loyer X, Rautou PE, Amabile N. Extracellular vesicles in coronary artery disease. Nat Rev Cardiol. 2017;14(5):259–72.
10. Chong SY, Lee CK, Huang C, Ou YH, Charles CJ, Richards AM, et al. Extracellular vesicles in cardiovascular diseases. Int J Mol Sci. 2019;20(13):3272.
11. de Hoog VC, Timmers L, Schoneveld AH, Wang JW, van de Weg SM, Sze SK, et al. Serum extracellular vesicle proteins and acute coronary syndrome. Eur Heart J Acute Cardiovasc Care. 2013;2(1):53–60.
12. Zhang YN, Vernooij F, Ibrahim I, Ooi S, Gijsberts CM, Schoneveld AH, et al. Extracellular vesicle proteins correlate with heart failure. PLoS ONE. 2016;11(2):e0148073.
13. Huang C, Neupane YR, Lim XC, Shekhani R, Czarny B, Wacker MG, et al. Extracellular vesicles in cardiovascular disease. Adv Clin Chem. 2021;103:47–95.

14. Min PK, Kim JY, Chung KH, Lee BK, Cho M, Lee DL, et al. Microparticles in STEMI culprit arteries. Atherosclerosis. 2013;227(2):323–8.
15. Porto I, Biasucci LM, De Maria GL, Leone AM, Niccoli G, Burzotta F, et al. Intracoronary microparticles and microvascular obstruction. Eur Heart J. 2012;33(23):2928–38.
16. Gąsecka A, van der Pol E, Nieuwland R, Stępień E. Extracellular vesicles in post-infarct remodeling. Kardiol Pol. 2018;76(1):69–76.
17. Waldenström A, Ronquist G. Role of exosomes in myocardial remodeling. Circ Res. 2014;114(2):315–24.
18. Koganti S, Eleftheriou D, Brogan PA, Kotecha T, Hong Y, Rakhit RD. Microparticles in coronary artery disease. Int J Cardiol. 2017;230:339–45.
19. Biasucci LM, Porto I, Di Vito L, De Maria GL, Leone AM, Tinelli G, et al. Microparticle release in ACS and stable angina. Circ J. 2012;76(9):2174–82.
20. Cui Y, Zheng L, Jiang M, Jia R, Zhang X, Quan Q, et al. Circulating microparticles in coronary heart disease. Mol Biol Rep. 2013;40(11):6437–42.
21. Boulanger CM, Scoazec A, Ebrahimian T, Henry P, Mathieu E, Tedgui A, et al. Microparticles cause endothelial dysfunction. Circulation. 2001;104(22):2649–52.
22. Kanhai DA, Visseren FLJ, van der Graaf Y, Schoneveld AH, Catanzariti LM, Timmers L, et al. Microvesicle proteins and vascular risk. Int J Cardiol. 2013;168(3):2358–63.
23. Wang JW, Zhang YN, Sze SK, van de Weg SM, Vernooij F, Schoneveld AH, et al. Dextran sulphate lowers procoagulant EVs. Int J Mol Sci. 2017;19(1):94.
24. Chan MY, Koh KWL, Poh SC, Marchesseau S, Singh D, Han Y, et al. IMMACULATE randomized clinical trial. JAMA Cardiol. 2021;6(7):830–9.
25. Lim XC, Yatim SMJM, Chong SY, Wang X, Tan SH, Yang X, et al. Plasma tissue factor activity post-MI. Front Endocrinol (Lausanne). 2022;13:1008329.
26. DeLong ER, DeLong DM, Clarke-Pearson DL. Comparing correlated ROC curves. Biometrics. 1988;44(3):837–45.
27. Boulet J, Mehra MR. Left ventricular reverse remodeling. Struct Heart. 2021;5(4):466–81.
28. Burchfield JS, Xie M, Hill JA. Pathological ventricular remodeling. Circulation. 2013;128(4):388–400.
29. Levin HR, Oz MC, Chen JM, Packer M, Rose EA, Burkhoff D. Reversal of chronic ventricular dilation in patients with end-stage cardiomyopathy by prolonged mechanical unloading. Circulation. 1995;91(11):2717–20.
30. Kim GH, Uriel N, Burkhoff D. Reverse remodelling and myocardial recovery in heart failure. Nat Rev Cardiol. 2018;15(2):83–96.
31. Matkovich SJ, Van Booven DJ, Youker KA, Torre-Amione G, Diwan A, Eschenbacher WH, et al. Reciprocal regulation of myocardial microRNAs and mRNA in human cardiomyopathy. Circulation. 2009;119(9):1263–71.
32. Yang KC, Yamada KA, Patel AY, Topkara VK, George I, Cheema FH, et al. Deep RNA sequencing reveals regulation of myocardial noncoding RNAs. Circulation. 2014;129(9):1009–21.
33. Ramani R, Vela D, Segura A, McNamara D, Lemster B, Samarendra V, et al. MicroRNA signature associated with recovery from assist device support. J Am Coll Cardiol. 2011;58(22):2270–8.
34. Mann DL, Barger PM, Burkhoff D. Myocardial recovery and the failing heart. J Am Coll Cardiol. 2012;60(24):2465–72.
35. Vischer UM. von Willebrand factor, endothelial dysfunction, and cardiovascular disease. J Thromb Haemost. 2006;4(6):1186–93.
36. Wang JW, Eikenboom J. von Willebrand disease and Weibel-Palade bodies. Hamostaseologie. 2010;30(3):150–5.
37. Kim JY, Aoki N, Abe S, Ichikawa N, Yoshida M, Nagaoka Y, et al. Plasma concentration of von Willebrand factor in acute myocardial infarction. Thromb Haemost. 2000;84(2):204–9.
38. Pendu R, Terraube V, Christophe O, Gahmberg C, de Groot PG, Lenting P, et al. P-selectin glycoprotein ligand-1 and β2-integrins in leukocyte adhesion. Blood. 2006;108(12):3746–52.
39. Koivunen E, Ranta TM, Annila A, Taube S, Uppala A, Jokinen M, et al. Inhibition of β2-integrin–mediated leukocyte adhesion. J Cell Biol. 2001;153(5):905–16.
40. Rosenberg RD. Biochemistry of heparin–antithrombin interactions. Am J Med. 1989;87(3 Suppl 1):S2–S9.
41. Horie S, Ishii H, Kazama M. Heparin-like glycosaminoglycan as a receptor for antithrombin III. Thromb Res. 1990;59(6):895–904.
42. Sniecinski RM, Welsby IJ, Levi M, Levy JH. Antithrombin: anti-inflammatory properties and clinical applications. Thromb Haemost. 2016;115(4):712–28.
43. Kim J. Annexin II: a plasminogen–plasminogen activator co-receptor. Front Biosci. 2002;7:d341–8.
44. Madureira PA, Surette AP, Phipps KD, Taboski MAS, Miller VA, Waisman DM. Role of annexin A2 heterotetramer in vascular fibrinolysis. Blood. 2011;118(18):4789–97.

45. Millien VO, Lu W, Shaw J, Yuan X, Mak G, Roberts L, et al. Cleavage of fibrinogen elicits allergic responses via TLR4. Science. 2013;341(6147):792–6.
46. Stewart AG, Xia YC, Harris T, Royce S, Hamilton JA, Schuliga M. Plasminogen-stimulated airway smooth muscle proliferation. Br J Pharmacol. 2013;170(7):1421–35.
47. Majumdar M, Tarui T, Shi B, Akakura N, Ruf W, Takada Y. Plasmin-induced migration via PAR-1 and integrin α9β1. J Biol Chem. 2004;279(36):37528–34.
48. Cozma A, Orăşan O, Sâmpelean D, Fodor A, Vlad C, Negrean V, et al. Endothelial dysfunction in metabolic syndrome. Rom J Intern Med. 2009;47(2):133–40.
49. Meigs JB, Mittleman MA, Nathan DM, Tofler GH, Singer DE, Murphy-Sheehy PM, et al. Hyperinsulinemia and impaired hemostasis. JAMA. 2000;283(2):221–8.
50. Apostolova MH, Seaman CD, Comer DM, Yabes JG, Ragni MV. Hypertension in von Willebrand disease. Clin Appl Thromb Hemost. 2018;24(1):93–9.
51. Verbree-Willemsen L, Zhang YN, Gijsberts CM, Schoneveld AH, Wang JW, Lam CSP, et al. LDL extracellular vesicle proteins after statin therapy. Int J Cardiol. 2018;271:247–53.
52. Shaw LJ, Merz CNB, Pepine CJ, Reis SE, Bittner V, Kelsey SF, et al. WISE study Part I. J Am Coll Cardiol. 2006;47(3 Suppl):S4–S20.
53. Merz CNB, Shaw LJ, Reis SE, Bittner V, Kelsey SF, Olson M, et al. WISE study Part II. J Am Coll Cardiol. 2006;47(3 Suppl):S21–9.
54. Gehrie ER, Reynolds HR, Chen AY, Neelon BH, Roe MT, Gibler WB, et al. NSTEMI with nonobstructive CAD. Am Heart J. 2009;158(4):688–94.
55. Shaw LJ, Bugiardini R, Merz CNB. Women and ischemic heart disease. J Am Coll Cardiol. 2009;54(17):1561–75.
56. Albrektsen G, Heuch I, Løchen ML, Thelle DS, Wilsgaard T, Njølstad I, et al. Lifelong gender gap in myocardial infarction risk. JAMA Intern Med. 2016;176(11):1673–9.